Cell Calcium 94 (2021) 102363

Contents lists available at ScienceDirect

Cell Calcium

journal homepage: www.elsevier.com/locate/ceca

Targeted Gq-GPCR activation drives ER-dependent calcium oscillations in chondrocytes

Ryan C. McDonough, Rachel M. Gilbert, Jason P. Gleghorn, Christopher Price *

Department of Biomedical Engineering, University of Delaware, United States

ARTICLE INFO

Keywords:
Chondrocyte
Calcium signaling
Designer receptors exclusively activated by Designer drugs
Chemogenetics
G protein coupled receptor activation

ABSTRACT

The temporal dynamics of calcium signaling are critical regulators of chondrocyte homeostasis and chondrogenesis. Calcium oscillations regulate differentiation and anabolic processes in chondrocytes and their precursors. Attempts to control chondrocyte calcium signaling have been achieved through mechanical perturbations and synthetic ion channel modulators. However, such stimuli can lack both local and global specificity and precision when evoking calcium signals. Synthetic signaling platforms can more precisely and selectively activate calcium signaling, enabling improved dissection of the roles of intracellular calcium ($[Ca^{2+}]_i$) in chondrocyte behavior. One such platform is hM3Dq, a chemogenetic DREADD (Designer Receptors Exclusively Activated by Designer Drugs) that activates calcium signaling via the $G\alpha_q$-PLCβ-IP_3-ER pathway upon administration of clozapine N-oxide (CNO). We previously described the first-use of hM3Dq to precisely mediate targeted, synthetic calcium signals in chondrocyte-like ATDC5 cells. Here, we generated stably expressing hM3Dq-ATDC5 cells to investigate the dynamics of $G\alpha_q$-GPCR calcium signaling in depth. CNO drove robust calcium responses in a temperature- and concentration-dependent (1 pM–100 μM) manner and elicited elevated levels of oscillatory calcium signaling above 10 nM. hM3Dq-mediated calcium oscillations in ATDC5 cells were reliant on ER calcium stores for both initiation and sustenance, and the downregulation and recovery dynamics of hM3Dq after CNO stimulation align with traditionally reported GPCR recycling kinetics. This study successfully generated a stable hM3Dq cell line to precisely drive $G\alpha_q$-GPCR-mediated and ER-dependent oscillatory calcium signaling in ATDC5 cells and established a novel tool to elucidate the role that GPCR-mediated calcium signaling plays in chondrocyte biology, cartilage pathology, and cartilage tissue engineering.

1. Introduction

Chondrocytes, the resident cell population within articular cartilage, are responsible for maintaining tissue health and homeostasis in response to both mechanical loads and soluble signaling factors [1]. Despite being characterized as non-excitable cells, one factor common in the response of chondrocytes to such stimuli is the reliance on calcium (Ca^{2+}) as a second messenger [2,3]. Chondrocytes, and their precursors, exhibit a range of intracellular Ca^{2+} ($[Ca^{2+}]_i$) signaling behaviors, and the modulation of these $[Ca^{2+}]_i$ signals are critical to the regulation of chondrogenesis [4–6], differentiation [7,8], cell survival [9,10] and the metabolic responses necessary for the proper development [11], maintenance [12], and engineering of cartilage tissue [3,13].

In general, chondrocyte $[Ca^{2+}]_i$ signaling is mediated by ion channels and receptors that drive cytosolic Ca^{2+} increases through Ca^{2+} influx from the extracellular space and/or intracellular stores [14,15]. Several mechanosensory pathways have been implicated in mechanically-induced $[Ca^{2+}]_i$ signaling within chondrocytes (e.g. compression, shear, fluid flow, hydrostatic pressure, and osmotic load-driven) [16–19]. Predominately, these mechanical perturbations activate the transient receptor potential vanilloid 4 (TRPV4) ion channel through membrane stretch [20,21]. However, a number of endogenous signaling compounds also regulate chondrogenic processes via their ability to modulate $[Ca^{2+}]_i$ signaling through ion channels, G-protein coupled receptors (GPCRs), tyrosine kinase receptors, etc [22–,23,24]. Additionally, pharmacological agents have been developed to specifically target endogenous Ca^{2+}-regulating transducers with the goal of activating chondrocyte $[Ca^{2+}]_i$ signaling for basic science, disease modifying, and tissue engineering purposes (4α-PDD, RN1734, and GSK1016790A are examples that signal through TRPV4 activation) [20]. Lastly, chondrocytes (and their precursors) exhibit spontaneous $[Ca^{2+}]_i$ signaling behaviors in the absence of external perturbations

* Corresponding author at: 161 Colburn Lab., University of Delaware, Newark, DE, 19716, United States.
E-mail addresses: ryancmcd@udel.edu (R.C. McDonough), rgilbert@udel.edu (R.M. Gilbert), gleghorn@udel.edu (J.P. Gleghorn), cprice@udel.edu (C. Price).

https://doi.org/10.1016/j.ceca.2021.102363
Received 3 December 2020; Received in revised form 18 January 2021; Accepted 24 January 2021
Available online 30 January 2021

[25].

One recently discovered regulator of chondrogenesis and chondrocyte homeostasis is oscillatory $[Ca^{2+}]_i$ signaling. Healthy chondrocytes and their precursors exhibit robust oscillatory Ca^{2+} signaling behaviors [11,26]. High-frequency, high-amplitude Ca^{2+} oscillations support differential regulation of effector proteins and transcription factors that encode complex chondrogenic signaling behaviors [27–30]. During cartilage development, high-frequency Ca^{2+} oscillations are associated with increased SOX9 expression, cell proliferation, and extracellular matrix production [31–34]. Stimulation of oscillatory Ca^{2+} signaling through TRPV4 activation accelerates collagen deposition by mesenchymal stem cells adhered to aligned patterned surfaces [35]. Ca^{2+} oscillations have also been detected in mature chondrocytes in response to a variety of exogenous stimuli and tend to promote matrix anabolism over catabolism, and enhancement of mechanical properties [36–39]. These underlying oscillatory $[Ca^{2+}]_i$ signaling behaviors are reliant upon intracellular Ca^{2+}stores [40], and are modulated by numerous regulatory mechanisms (i.e., Ca^{2+} pump activity, Ca^{2+} store refilling, signaling molecule metabolism and recycling, protein binding, etc.) [2,41–44].

Collectively, the literature clearly establishes the importance of $[Ca^{2+}]_i$ signaling dynamics in the proper control of cartilage development, chondrocyte adaptation and homeostasis, and that experimentally controlling dynamic Ca^{2+} signaling in chondrocytes can enhance biosynthetic and material property outcomes in native and engineered cartilage [3,13,15,45,46]. And while the field of chondrocyte biology has sought to leverage control of different endogenous signaling pathways to interrogate the influence of $[Ca^{2+}]_i$ signaling pathways on chondrogenesis, cartilage development, and chondrocyte/cartilage homeostasis [3,13,15,45], such 'physiologically-mediated' $[Ca^{2+}]_i$ manipulations are restricted to a rather small range of targets for which there exists concerns over specificity and precision. For example, mechanical stimulation can target multiple mechanosensitive components simultaneously, some of which are not Ca^{2+} selective [47,48], while the use of biomolecules, both synthetic (e.g. GSK101) or natural (e.g. Histamine, PTH, etc.), to target endogenous signaling pathways carries the risk of significant off-target effects [49,50].

To overcome such limitations, and to more precisely dissect the role of specific Ca^{2+}-mediated signaling processes in chondrocyte biology, we recently described the use of a chemogenetic platform, termed designer receptors exclusively activated by designer drugs (DREADD), to drive $[Ca^{2+}]_i$ signaling in a chondrocyte-like cell line in a highly-specific, and fully-synthetic manner [51]. DREADDs encompass a family of engineered G-protein coupled receptors (GPCRs) molecularly evolved to exhibit significantly greater affinity for the pharmacologically inert compound, clozapine*N*-oxide (CNO), than their native endogenous ligand, acetylcholine [52]. GPCRs signal through second messenger pathways associated with four G-protein alpha subunits (i.e. $G\alpha_s$, $G\alpha_{q/11}$, $G\alpha_{12/13}$, and $G\alpha_i$), which together constitute the largest family of membrane-bound signal transduction proteins and represent ~34 % of all clinical drug targets [53–56]. DREADDs for $G\alpha_s$-, $G\alpha_i$-, and $G\alpha_q$-coupled GPCRs have been developed based off of mammalian metabotropic (muscarinic) cholinergic receptors [57]. $G\alpha_s$ (rM3Ds) and $G\alpha_i$ (hM4Di/KORD) DREADDs indirectly modulate $[Ca^{2+}]_i$ signaling through the adenyl cyclase-cyclic AMP (cAMP) pathway [58]. In contrast, hM3Dq (a $G\alpha_q$ DREADD) can directly regulate $[Ca^{2+}]_i$ signaling through the ubiquitous $G\alpha_q$-PLCβ-IP_3 pathway and IP_3-mediated release of Ca^{2+} from the endoplasmic reticulum (ER) [59]. This pathway is one of the most commonly utilized calcium release mechanisms in cells [60], and is intimately associated with chondrocyte mechanotransduction [61] and oscillatory $[Ca^{2+}]_i$ signaling behaviors [62]. Thus, hM3Dq represents an innovative tool for specifically and synthetically regulating GPCR-dependent $[Ca^{2+}]_i$ signaling, and $G\alpha_q$-dependent signaling more generally, having been leveraged with transformative success in the neurological sciences [63,64] and to control the metabolic activity of a number of non-neuronal cell types (e.g., liver, kidney, pancreas) [65–67].

Our previous work established the ability of hM3Dq to safely drive CNO-mediated activation of $[Ca^{2+}]_i$ signals within chondrocyte-like ATDC5 cells and represented the first application of chemogenetic approaches to musculoskeletal tissues [51]. However, that study utilized transient transfection of an HA-tagged protein, which supported only moderate (~40 % efficacy), short-term expression of the hM3Dq protein (~5 days), limiting the ability to conduct long-term studies of hM3Dq-mediated Ca^{2+} activation on chondrocyte metabolism/homeostasis. In the present study, we address these limitations by generating an ATCD5 cell line stably expressing a mCherry-tagged hM3Dq and leveraged it to analyze CNO-mediated Ca^{2+} signaling behaviors. Critically, we identified that CNO could drive, in a dose- and temperature-dependent manner, the coordinated and widespread generation of rapid primary $[Ca^{2+}]_i$ peaks in hM3Dq cells, which were subsequently followed by sustained, cell-autonomous oscillatory Ca^{2+} signals in a high percentage of hM3Dq cells, and were reliant upon ER Ca^{2+} refilling and PLCβ-driven IP_3 generation/modulation. Overall, this work demonstrated the facile ability to precisely and synthetically drive $G\alpha_q$-PLCβ-IP_3-dependent signaling cascades and induce ER-dependent Ca^{2+} release through activation of the hM3Dq DREADD in chondrocyte-like cells, providing a novel platform for studying GPCR function and Ca^{2+} signaling within chondrocytes and their precursors.

2. Methods

2.1. Stable hM3Dq-mCherry-ATDC5 cell line generation

hM3Dq-mCherry was cloned out of the pAAV-Tight-PTRE-hM3Dq-mCherry plasmid (Addgene, #66795) and into a pCDH-CMV-MCS-EF1α-Puro lentiviral vector (Systems Bioscience Inc.) [performed by Aldevron, Fargo, ND] (Fig. 1A). The resulting lentiviral construct, pCDH-CMV-hM3Dq-mCherry-EF1α-Puro, was co-transfected into HEK293TN cells (cultured in 1:1 Dulbecco's Modified Eagle Medium/Ham's F12K [DMEM/F12] + 10 % fetal bovine serum [FBS] + 1X penicillin-streptomycin [PS]) with the necessary lentiviral packaging and envelope plasmids, psPAX2 and pCMV-VSV-G (Addgene, #12260 and #8454, respectively), to create hM3Dq-mCherry lentiviral particles (Fig. 1B). Viral particles were collected and used immediately for transduction or stored at −80 °C. Chondrogenic ATDC5 cells (Lonza) were cultured in complete growth media (consisting of 1:1 DMEM/F12, 5% FBS, 1X PS) for 72-hs before lentiviral transduction. ATDC5 cells were transduced for 24 -hs, hM3Dq-mCherry expression confirmed via fluorescence microscopy and assessment of CNO-stimulated Ca^{2+} response, and polyclonal populations of ATDC5-hM3Dq-mCherry cells ($hM3Dq^+$) were generated and maintained via continuous puromycin selection (10 μg/mL) (Fig. 1C).

2.2. Image acquisition and experimental design

Cells were plated in coverglass-bottom dishes at 10,000 cells/cm^2 24-hs prior to Ca^{2+} imaging. Samples were stained with 5μM Fluo-8AM + 0.02 % Pluronic F-127 for 30 min at 37 °C, washed 3x in Hank's Basic Salt Solution (HBSS) and transferred to a Zeiss AxioObserver.Z1 Apotome.2 with a temperature-controlled incubation chamber. Each sample was imaged for 15-min, with the first 5-min used to establish baseline signaling, before pharmacological stimulation was applied, and the subsequent CNO-mediated response over the remaining 10 min. Imaging was performed at 25 °C and 37 °C for the dose response experiments, and at 37 °C for all other experiments. All studies were performed in Ca^{2+} replete media unless noted otherwise.

2.2.1. CNO dose response

$hM3Dq^+$ cells and wild-type (WT) ATDC5 cells were stimulated with a single dose of CNO diluted in HBSS at concentrations ranging from 1 pM to 100 μM (10^{-12}–10^{-4} M). From this data a dose curve was

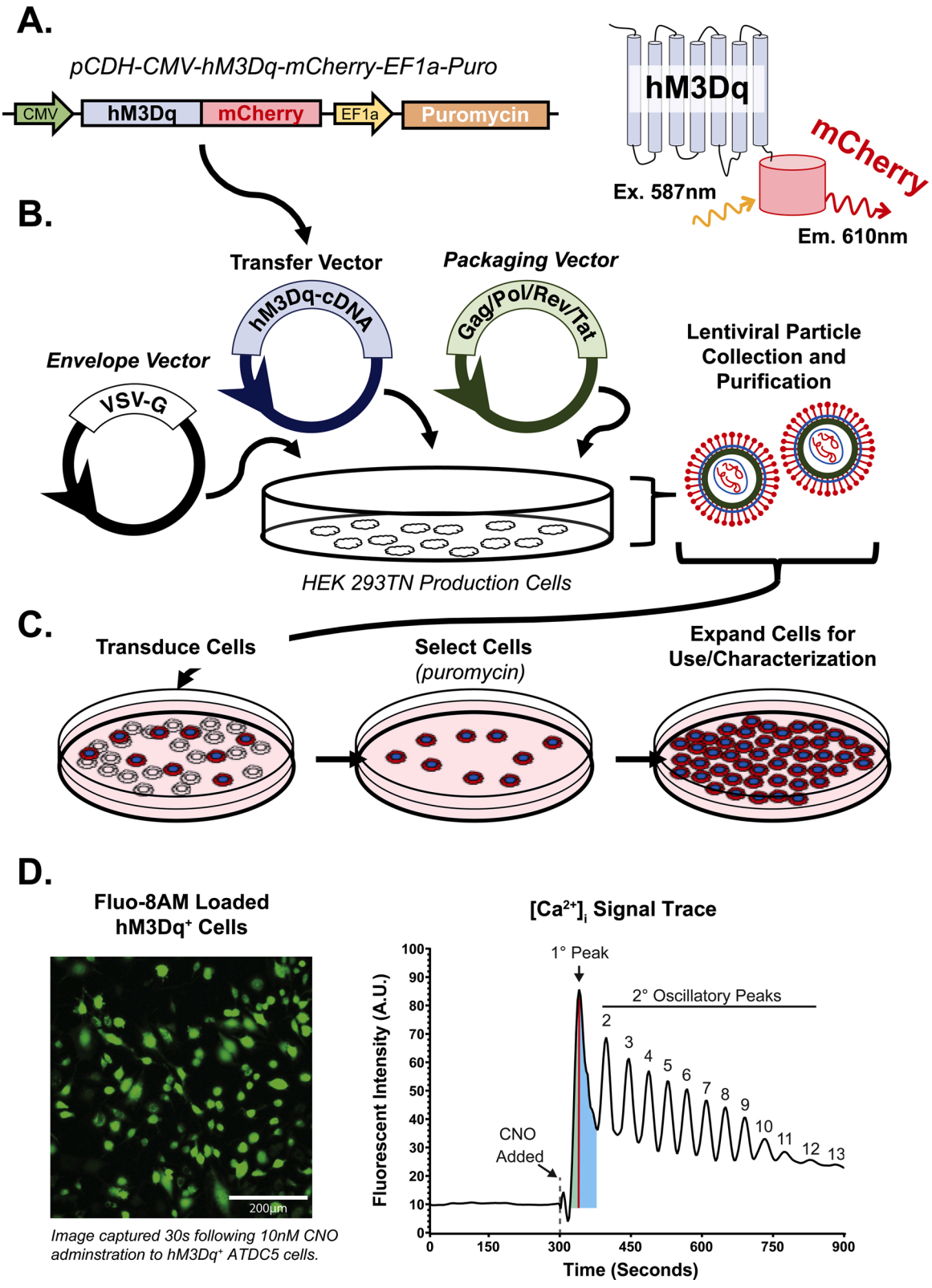

(caption on next page)

Fig. 1. Stable hM3Dq-mCherry-ATDC5 Cell Line Generation and Ca^{2+} signal analysis. **A.** The hM3Dq-mCherry DREADD receptor was cloned out of the pAAV-Tight-PTRE-hM3Dq-mCherry plasmid and into the pCDH-CMV-MCS-EF1α-Puro lentiviral vector via restriction enzyme digest. **B.** The resulting pCDH-CMV-hM3Dq-mCherry-EF1α-Puro lentiviral construct was co-transfected into HEK293TN cells with psPAX2 and pCMV-VSV-G lentiviral packaging and envelope plasmids using PureFection Transfection Reagent. **C.** hM3Dq-mCherry lentiviral particles were collected and transduced onto ATDC5 cells for 24 h. hM3Dq-mCherry expression was confirmed via fluorescence microscopy and subsequent assessment of CNO-stimulated Ca^{2+} response, and polyclonal populations of ATDC5-hM3Dq-mCherry cells ($hM3Dq^+$ cells) were generated via continuous selection with 10 μg/mL puromycin. **D.** A representative Fluo-8AM Ca^{2+} signal trace for a $hM3Dq^+$ ATDC5 cell highlighting the CNO-evoked primary (1°; i.e., the first detected Ca^{2+} peak after CNO administration) and secondary (2°; subsequent peaks/oscillations) $[Ca^{2+}]_i$ signaling behaviors. Peak start and end times were defined as the timepoint three frames to the right, or left, of each peak's 'threshold' inflection point, respectively; peak duration was defined as the time between peak end- and start-times. Peak rise (green shading) and fall (blue shading) times were calculated with respect to the maximal peak intensity timepoint. Peak height (red line) was defined as the total height relative to the intensity at the peak start timepoint. Inter-peak period was defined as the time between the maximal signal intensities for two 'neighboring' peaks. Often, after the addition of CNO (at 300 s), a minor fluctuation in fluorescent signal was observed due to optical aberrations, but these could be easily distinguished from the CNO-evoked Ca^{2+} signaling behaviors. An inset of Fluo-8AM stained $hM3Dq^+$ ATDC5 cells captured approximately 30 s following CNO administration illustrates the widespread and coordinated eliciting of $[Ca^{2+}]_i$ signaling within $hM3Dq^+$-cells by CNO.

constructed and the EC_{50} was determined. Subsequent studies were performed at concentrations ranging from ~1 to ~200-times the EC_{50} concentration (1X to 200X respectively). Additional samples were exposed to either 10 nM GSK101 (ThermoFisher), or 50 % hypo-osmotic shock (50 % dilution of HBSS with deionized water), since both up-regulate Ca^{2+} entry into ATDC5 cells through mechanisms involving the Ca^{2+} channel TRPV4 (GSK101 is a small molecule agonist of TRPV4, and hypo-osmotic shock via membrane stretch activation of TRPV4 and calcium-induced-calcium-release) [17,45,68].

2.2.2. Ca^{2+} signaling pathway inhibition

To identify intra/intercellular signaling pathway contributors to the initial and oscillatory Ca^{2+} signaling behaviors of CNO-activated cells, $hM3Dq^+$ cells were incubated with a variety of inhibitors targeting $G\alpha_q$- and paracrine-mediated Ca^{2+} signaling pathways. For targeted intracellular pathway inhibition: 10 μM Xestospongin C (IP_3 receptor antagonist, Cayman Chemical; AnnArbor, MI), 1 μM thapsigargin (sarco/endoplasmic reticulum Ca^{2+}-ATPase [SERCA] antagonist, Cayman Chemical), 10 μM GF109203X (PKC antagonist, Enzo Life Sciences; Farmingdale, NY), 10 μM U-73122 (PLCβ antagonist, Tocris) were utilized. Inhibitors were applied 30-minutes prior to stimulation with 200X CNO. Because pre-inhibition of $hM3Dq^+$ cells with thapsigargin completely abolishes hM3Dq-mediated ER Ca^{2+} release [69], we performed a timed inhibition study, in which thapsigargin or U-73122 was applied 'simultaneously' with 200X CNO; *nota bene*: in these 'simultaneous' studies, inhibitors were applied 10 s following CNO addition to limit their influence on the primary CNO-evoked ER Ca^{2+} release. For targeted intercellular pathway assessment: 10 μM Apyrase (ATP/ADP hydrolysis, Sigma), 10 μM PPADS (P2X receptor antagonist, Tocris), 10 μM AR-C 118925XX (P2Y receptor antagonist, Tocris), Ca^{2+}-free HBSS (extracellular calcium depletion, Sigma), 5 μM gadolinium chloride (non-selective calcium channel antagonist, Sigma), and 10 μM GSK205 (TRPV4 antagonist, EMD Millipore; Burlington, MA) were utilized. Additionally, $[Ca^{2+}]_i$ responses were assessed in a 'mixed' population of cells consisting of $hM3Dq^+$ cells and WT-ATDC5 cells (mixed at a 1:1 ratio) to interrogate paracrine-based Ca^{2+} signal activation of non-hM3Dq-mCherry-expressing cells following activation of $hM3Dq^+$ cells.

2.2.3. Refractory behavior

To identify the time course for reactivation of Ca^{2+} signaling in $hM3Dq^+$ cells following CNO activation (i.e., their refractory behavior) cells were first stimulated with CNO and imaged as described above. Cells were then washed twice with fresh HBSS, and re-stimulated 15-min, 30-min, 1-h, 4-hs, or 24-hs after the first CNO dose; this process was repeated for a third dosing.

2.3. Signal and data analysis

A custom MATLAB program was developed to extract $[Ca^{2+}]_i$ signals from individual cells within each image series (Fig. 1D). A calcium peak was defined as an increase in a cell's Fluo-8AM fluorescence intensity greater than 3 standard deviations its baseline (average of first 5-minutes) fluorescence. The population response was defined as the percentage of cells exhibiting at least one calcium peak following stimulation. From these Ca^{2+} signals, the first peak detected immediately after addition of CNO was identified as the primary CNO Ca^{2+} response, and all subsequent peaks were labeled as secondary or oscillatory responses. The percentage of cells responding with 1 peak, ≥2 peaks, and ≥9 peaks after stimulation, and the temporal properties (peak duration, rise, fall, and period times, and amplitude) of each calcium peak were determined. Statistical analysis was performed in GraphPad Prism v8 (GraphPad Software; La Jolla, CA). Data outliers were identified using the ROUT method (robust regression and outlier removal) [70]. *t*-tests, one-way (single CNO stimulation) and two-way ANOVAs (repeated CNO stimulation) with Tukey's post-hoc tests, and regression analysis (linear and non-linear) were performed where appropriate. All data are presented as mean ± range. The threshold for statistical significance was set at a multiplicity correct *p*-value of $p < 0.05$.

3. Results

3.1. Confirmation of stable hM3Dq-mCherry expression in ATDC5 cells

Fluorescent visualization of mCherry-tagged hM3Dq confirmed successful expression of hM3Dq in ATDC5 cells following transduction; mCherry signals were not observed in non-transduced (WT) ATDC5 cells (Fig. 2A & B). ~97 % of transduced and continuously selected cells expressed hM3Dq-mCherry (versus 0% in WT cells, Fig. 2C; 193.8 ± 95.7 cells/replicate, n = 3 replicates/cell line; cells shown at 10 days post-transduction). Structured illumination microscopy (STIM) confirmed both diffuse membrane localization and punctate clustering of mCherry-hM3Dq in $hM3Dq^+$ cells (Fig. 2D).

3.2. Population dynamics of CNO-mediated Ca^{2+} responses in $hM3Dq^+$ cells

In the absence of CNO, WT cells and $hM3Dq^+$ cells exhibited infrequent, spontaneous activations of $[Ca^{2+}]_i$ signaling (Fig. 3A, Supplemental Video 1; ~1% to 12 % of cells), and limited oscillatory Ca^{2+} signaling behaviors (less than 1% showed >1 Ca^{2+} peak; Fig. 3B). Treatment of WT cells with CNO did not alter Ca^{2+} signaling behaviors. It is noteworthy that in WT cells, spontaneous Ca^{2+} signaling was slightly higher at 37 °C than 25 °C, consistent with temperature-dependent effects on chondrocyte Ca^{2+} signaling [71,72].

In contrast, $hM3Dq^+$ cells stimulated with CNO exhibited robust $[Ca^{2+}]_i$ activation, eliciting immediate primary Ca^{2+} activation peaks typically followed by oscillatory Ca^{2+} signaling (Supplemental Video 2). The percentage of $hM3Dq^+$ cells that evoked a primary, CNO-mediated Ca^{2+} peak increased in a dose-dependent manner at 25 °C and 37 °C (Fig. 3A; 136.5 ± 32.7 cells/experiment), with EC_{50}'s of ~5.1 nM and

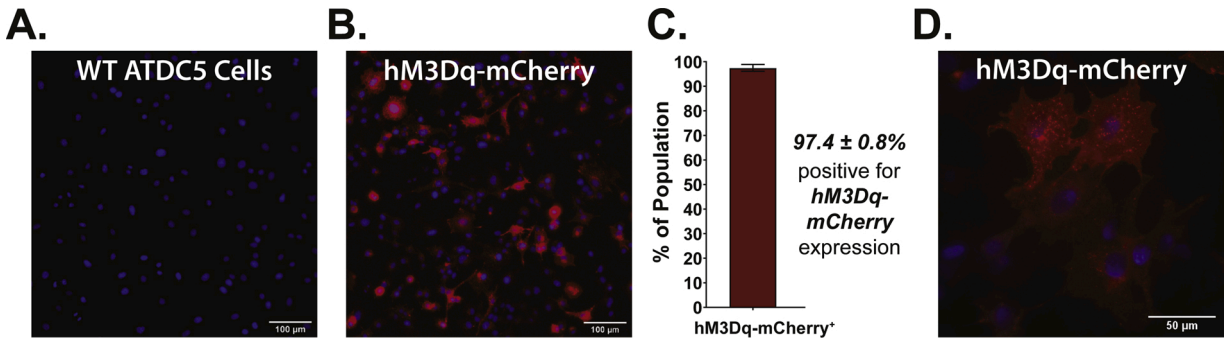

Fig. 2. A. Wild-type (WT) ATDC5 cells exhibited no detectable expression of hM3Dq-mCherry receptor protein. **B.** Lentiviral-transduced ATDC5 cells exhibited robust hM3Dq-mCherry receptor protein expression; as assessed by the fluorescent imaging of the conjugated mCherry-reporter tag (**red**), cell nuclei are counter-stained with DAPI (**blue**). **C.** Quantification of hM3Dq-mCherry receptor protein expression by fluorescent imaging found >97 % of lentiviral transduced to be mCherry-hM3Dq positive (hM3Dq$^+$) following continuous puromycin selection ($p < 0.0001$, *t*-test; data presented as mean ± range). **D.** Super-resolution structured illumination microscopy (STIM) imaging (at 63x magnification) highlighted the plasma membrane and intracellular vesicle localization of the mCherry-hM3Dq receptor in hM3Dq$^+$ ATDC5 cells.

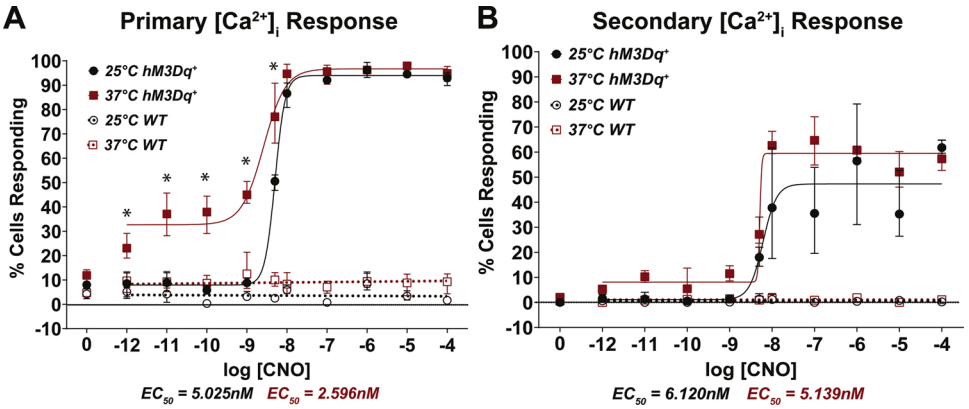

Fig. 3. A. Primary and **B.** Secondary $[Ca^{2+}]_i$ signaling responses evoked by CNO (10^{-12} to 10^{-4} M) in wild-type (WT) and hM3Dq$^+$ ATDC5 cells at 25 and 37° C. WT cells were irresponsive to CNO at all concentrations, exhibiting only infrequent spontaneous $[Ca^{2+}]_i$ activations. hM3Dq$^+$ cells exhibited classic population-level dose responses (i.e., largely sigmoidal) with regards to CNO-driven primary and secondary $[Ca^{2+}]_i$ peak generation. The EC_{50} for primary $[Ca^{2+}]_i$ peak generation was ~5.0 nM CNO at 25°C and ~2.6 nM CNO at 37°C in hM3Dq$^+$ cells, and the primary $[Ca^{2+}]_i$ peak response saturated at >95 % of hM3Dq$^+$ cells at both temperatures. The EC_{50} for secondary $[Ca^{2+}]_i$ signal generation (2^+ peaks) by CNO were ~6.1 nM at 25°C and ~5.1 nM at 37°C, and a slightly higher secondary $[Ca^{2+}]_i$ signal response was found at 37° C for high CNO concentrations ($<10^{-8}$ M). All data are presented as mean ± range. * indicates statistically significant difference between hM3Dq$^+$ response at 25°C and 37°C for the indicated CXNO concentration; $p < 0.05$, *t*-test.

~2.6 nM, respectively. While the percentage of responding cells saturated (>95 %) above 10 nM CNO for both 25 °C and 37 °C, their response diverged at low CNO concentrations. For <1 nM CNO, hM3Dq$^+$ cells displayed only infrequent spontaneous Ca^{2+} signaling at 25 °C (~10 % of cells), whereas the percentage of responding cells was significantly elevated at 37 °C (~24 % to 43 %). A dose-dependent effect was also observed for the percentage of cells exhibiting ≥2 peaks following CNO treatment (Fig. 3B). The EC_{50} for multiple Ca^{2+} responses were ~6.2 nM and ~5.1 nM for 25 °C and 37 °C, respectively, with a slightly higher percentage of cells exhibiting multiple responses at 37 °C. Maximal primary CNO-mediated Ca^{2+} activation in hM3Dq$^+$ cells were comparable to those elicited by GSK101 and 50 % hypo-osmotic shock stimulation—established activators of Ca^{2+} signaling in ATDC5 cells; however, these Ca^{2+} activators produced far smaller percentages of cells exhibiting oscillatory signaling behavior compared to CNO (Supplemental Fig. 1).

3.3. Temporal dynamics of CNO-mediated Ca^{2+} responses in hM3Dq$^+$ cells

Looking at Ca^{2+} signaling behaviors at 37 °C, CNO administration elicited extensive oscillatory Ca^{2+} signaling activities in hM3Dq$^+$ cells (Fig. 4). Below 10 nM, CNO administration evoked on average 1.5 Ca^{2+} peaks in responsive hM3Dq$^+$ cells, whereas under saturating CNO concentrations (10 nM-100 μM) the average number of Ca^{2+} peaks varied in a biphasic manner, increasing to a maximum number of oscillations at 0.1−1 μM before decreasing at higher CNO concentrations (Fig. 4A; in one case, 26 oscillations were observed over 10-minutes in a single cell following 1 μM CNO addition, see Fig. 4B & Supplemental Fig. 2). At 25 °C, the average number of Ca^{2+} peaks elicited by CNO increased in a linear manner with CNO concentration, to an average of ~2 (Supplemental Fig. 3). In all cases, the intensity of the primary CNO evoked Ca^{2+} peak (~35 a.u.) was larger than the intensity of subsequent peaks, and oscillatory peak heights diminished linearly with peak number (down to ~3 a.u.; Fig. 4B). WT cells administered similar CNO levels occasionally exhibited one (median value), and no more than three, spontaneous Ca^{2+} peaks, with peak intensities between ~10−15 a.u.

Analysis of the temporal dynamics of CNO-driven Ca^{2+} signaling in hM3Dq$^+$ cells revealed an inverse relationship between CNO concentration and primary Ca^{2+} peak duration (Supplemental Fig. 4A) and CNO evoked primary Ca^{2+} peaks tended to be of shorter duration at physiological temperatures (p <0.001, for slope). At the lowest concentration tested (10^{-12} M CNO) peak durations ranged from 225 s at 37 °C to 350 s at 25 °C, and decreased to ~50−100 s, respectively, at the

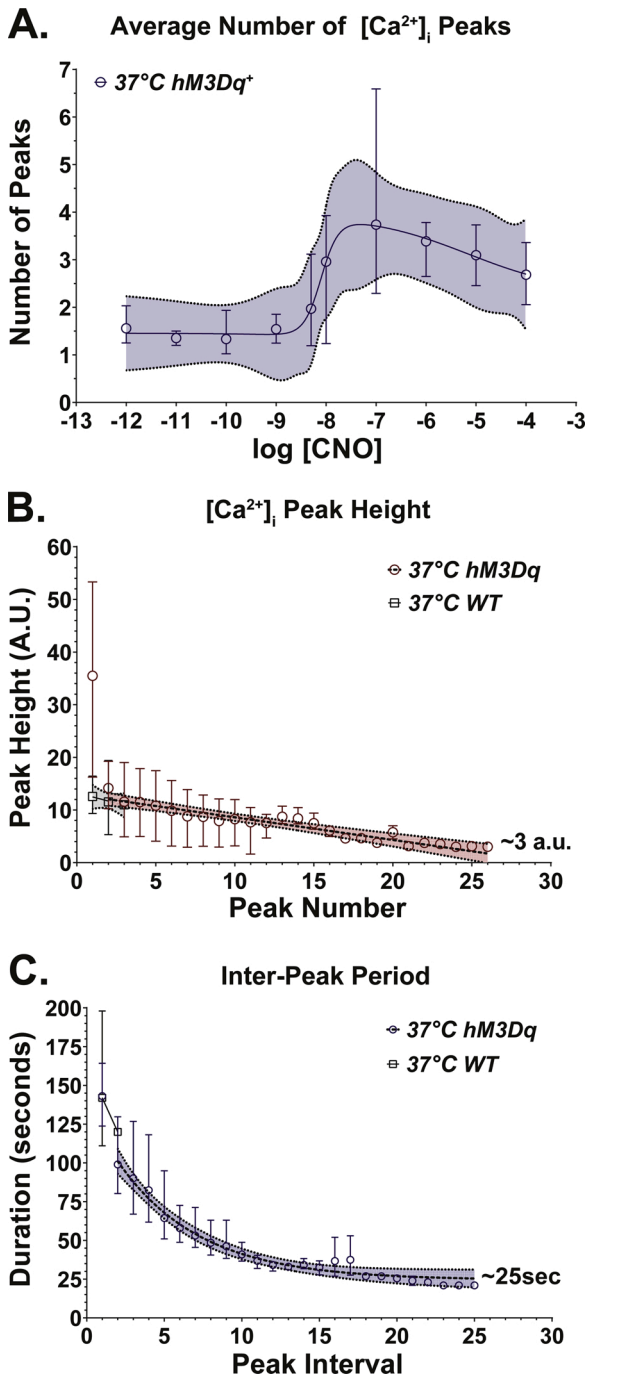

(caption on next column)

Fig. 4. Average CNO-activated Ca^{2+} responses **A.** Number of peaks elicited as a function of CNO dose. Below 10 nM, the number of peaks evoked by CNO administration to $hM3Dq^+$ ATDC5 cells appeared flat (~1 to 2 peaks per cell, average = ~1.5). Above 10 nM the number of peaks evoked showed a bi-phasic behavior, with a maximum average of ~3.5 per cell at 100 nM, then decreasing at higher CNO concentrations. **B.** $[Ca^{2+}]_i$ peak intensities as a function of evoked peak number After the induction of a very-large initial (i.e., primary) CNO-induced Ca^{2+} peak (~35 a.u.) in $hM3Dq^+$ ATDC5 cells, the intensity of subsequent oscillations (i.e., secondary peaks) decreased monotonically with peak number. In $hM3Dq^+$ cells, oscillatory $[Ca^{2+}]_i$ peak intensity dropped to ~3 a.u., or <10 % of the first peak's intensity. The intensity of $[Ca^{2+}]_i$ peaks in WT ATDC5 cells, which reflect only low-level spontaneous Ca^{2+} signaling, ranged from 10-15 a.u., and were consistent with the intensity of early CNO activated $[Ca^{2+}]_i$ oscillations in $hM3Dq^+$ cells. *Note:* The median number of Ca^{2+} peaks observed in WT cells was one (1), with a maximum of three (3). **C.** Inter-peak period (i.e., time between peaks) as a function of evoked peak interval. Average inter-peak period decreased monotonically in $hM3Dq^+$ cells with secondary/oscillatory peak number, from a maximum of ~140 s to a plateau of ~25 s. The peak periods noted on the graph correspond to the interval between two subsequent peaks (i.e., interval 2 = between peak 2 and 3). All data are presented as mean ± range, and the data fits shown as either spline (**A**), linear (**B**) or exponential decay (**C**) curves with their 95 % confidence intervals. Data for **B** and **C** were derived from CNO responsive $hM3Dq^+$ (or WT) cells across all testing concentrations.

highest CNO concentration (10^{-4} M). In contrast, spontaneous Ca^{2+} signaling dynamics appeared unaffected by CNO or temperature in WT cells, exhibiting consistent peak duration times of ~50−110 s. Similar quantitative behaviors were observed for the rise and fall times of the CNO-evoked primary Ca^{2+} peaks (Supplemental Fig. 5). In $hM3Dq^+$ cells, the temporal dynamics of oscillatory Ca^{2+} signaling were remarkably insensitive to CNO concentration (Supplemental Fig. 4B). On a population basis, the dynamics of Ca^{2+} signaling were far more variable at lower CNO concentrations (Supplemental Fig. 6). Following CNO administration, the average time between subsequent (oscillatory) Ca^{2+} peaks (period) decayed monotonically, from a maximum of ~140 s between the first and second peak to ~25 s between later peaks (Fig. 4C). Based upon these data, we chose a CNO concentration of 500 nM (200X), balancing high oscillatory peak induction percentages and oscillation numbers, to conduct further studies of CNO-evoked oscillatory Ca^{2+} signaling behavior in $hM3Dq^+$ ATDC5 cells at 37 °C.

3.4. Ca^{2+} signaling pathway inhibition

Inhibition of intracellular pathways implicated in $G\alpha_q$-mediated Ca^{2+} signaling downstream of hM3Dq (PLCβ, IP_3R, and ER-mediated Ca^{2+} storage/release) prior to 500 nM CNO addition abolished all hM3Dq-dependent Ca^{2+} responses, including both primary peak and oscillatory signaling; only infrequent spontaneous Ca^{2+} signaling was observed. However, when thapsigargin or U-73122 was applied simultaneously with CNO addition (and in the presence of extracellular Ca^{2+}), initial Ca^{2+} peaks were preserved, but all secondary oscillations abolished (Fig. 5A). Additionally, inhibition of PKC significantly reduced the number of multiple signaling events, but not primary Ca^{2+} activations (Fig. 5B, $p = 0.0536$).

Inhibition of putative intercellular signaling mechanisms in $hM3Dq^+$ cells (extracellular ATP signaling, P2Y [ATP-sensitive $G\alpha_q$-coupled GPCR], and P2X [ATP-sensitive cation channel] individually), were unable to prevent oscillatory signaling in response to 500 nM CNO (Fig. 5C). However, when these inhibitors were combined, significant reductions in the number of cells responding with ≥2 peaks and ≥9 peaks were observed, dropping from ~52 % to ~25−30%, and from ~14 % to ~3−5%, respectively. Removal of extracellular Ca^{2+}, broad inhibition of membrane Ca^{2+} channels, or inhibition of TRPV4 (an ion channel potentially regulated downstream of $G\alpha_q$-GPCR signaling), moderately suppressed the number of cells responding with ≥2 peaks (~55 % to ~34−41%), but not ≥9 peaks in $hM3Dq^+$ cells (Fig. 5D).

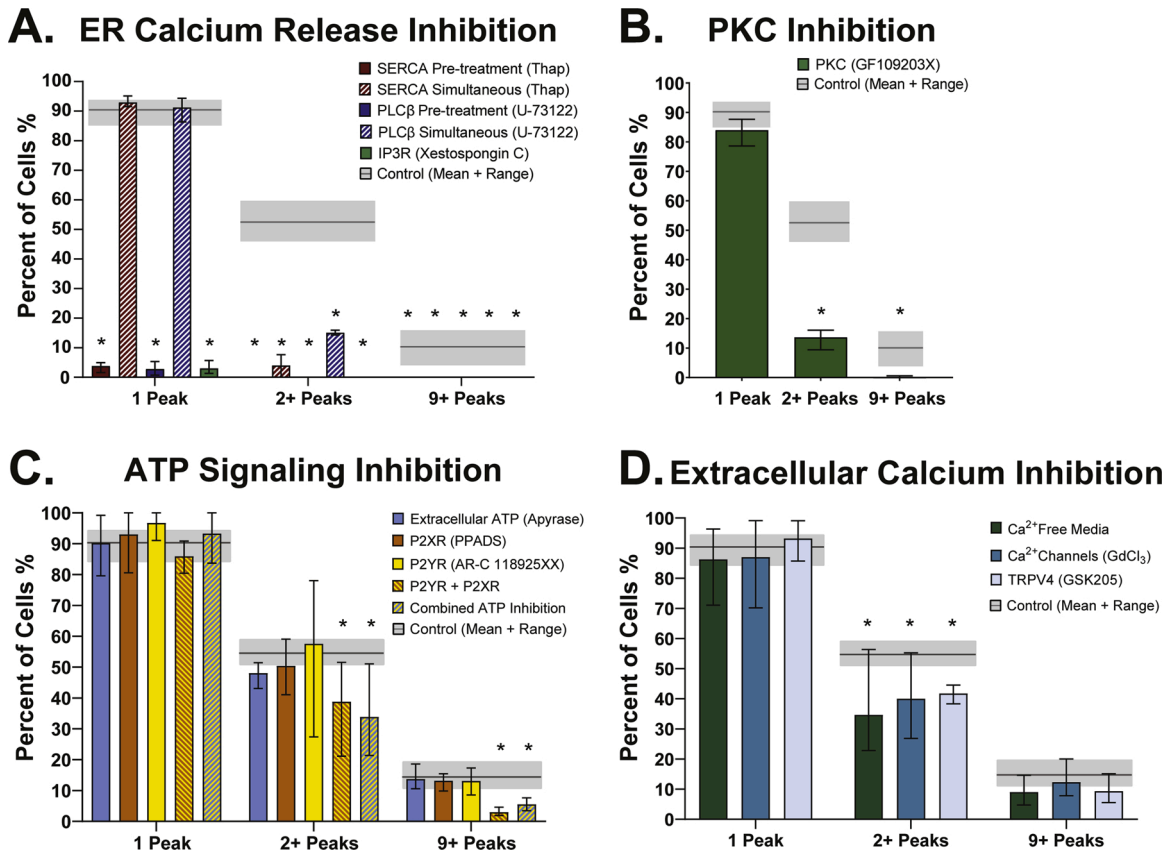

Fig. 5. Influence of Ca^{2+} signaling pathway inhibitors on CNO-evoked primary and secondary $[Ca^{2+}]_i$ signaling responses in $hM3Dq^+$ ATDC5 cells. In response to 500 nM CNO administration, >90 % of $hM3Dq^+$ cells elicited a CNO-driven primary Ca^{2+} peak, ~50 % two or more peaks, and ~14 % nine or more peaks (indicated as respective grey shaded regions in A-D). **A.** Pre-treatment of $hM3Dq^+$ cells with $G\alpha_q$-GPCR signaling pathway inhibitors (Thapsagargin, U-73122, or Xestospongin C) completely abolished Ca^{2+} responses elicited by CNO; however, simultaneous addition of such inhibitors with CNO only blocked subsequent CNO-mediated Ca^{2+} oscillations, but not the initial CNO Ca^{2+} peak. **B.** Pre-inhibition of PKC (GF109203X) attenuated CNO-mediated Ca^{2+} oscillations, but not primary CNO Ca^{2+} peaks. **C.** Inhibition of individual ATP signaling components (apyrase, PPADS, AR-C 118925XX) did not attenuate the CNO-mediated Ca^{2+} response or oscillatory signaling behaviors. However, combined inhibition of ATP receptor signaling significantly reduced the number of cells exhibiting two or more peaks ($p = 0.0154$ and 0.0361). **D.** Inhibition of extracellular calcium entry pathways did not attenuate CNO-mediated primary Ca^{2+} responses, but modestly attenuated the population of cells exhibiting 2^+, but not 9^+ peaks. All data are presented as mean ± range; the grey shaded region and their black lines indicate the respective data range and mean for the control $hM3Dq^+$ cells treated with 500 nM CNO. * indicates $p < 0.001$ compared to 500 nM CNO control; one-way ANOVA w/ Tukey post-hoc.

To confirm that Ca^{2+} oscillations observed upon CNO administration were not driven by paracrine signaling mediators, $hM3Dq^+$ cells were mixed 1:1 with WT cells and this mixed population stimulated with CNO at 37 °C. As expected, only 50 % of the cells in this mixed population expressed mCherry-hM3Dq (confirmed via fluorescence microscopy; Fig. 6A), and the population of cells that responded with primary peaks and oscillatory Ca^{2+} signaling in response to 2.5 nM (1xIC50) and 500 nM (200xIC50) CNO was reduced by 50 % relative to a pure $hM3Dq^+$ population (Fig. 6B, C). Only cells that were $mCherry^+$ (i.e., $hM3Dq^+$ cells; Fig. 6D, E) responded to CNO administration with coordinated $[Ca^{2+}]_i$ peaks and oscillations; WT cells only exhibited infrequent Ca^{2+} signals consistent with spontaneous Ca^{2+} activation.

3.5. Reactivation and refractory behaviors

Assessing the Ca^{2+} response of stably transduced $hM3Dq^+$ cells to sequential CNO washout and re-stimulation demonstrated a significant attenuation of CNO-mediated Ca^{2+} activation (refractory behavior) at short re-stimulation times (30-minutes or less; Fig. 7). At 5 (2X), 50 (20X), and 500 nM (200X) CNO, the percentage of cells reactivated by CNO 15 min after an initial stimulation was consistently less than 50 % of the initial response percentage ($p<0.0001$). Increasing the duration of the recovery period demonstrated that near-100 % recovery of coordinated hM3Dq-meidated signaling could be achieved following 1 h in the absence of CNO ($p > 0.5$, all concentrations), indicating a refractory period between 30 and 60 min.

4. Discussion

Directed activation of Ca^{2+} signaling in chondrocytes and their precursors via mechanical forces and soluble factor signaling constitute potent means of regulating chondrocyte proliferation, differentiation, homeostasis, matrix metabolism, and mechano-adaptation for both basic science and tissue engineering/regeneration purposes [3,24,73–75]. Numerous endogenous Ca^{2+} signal transduction mechanisms present targets for controlling chondrocyte gene expression, matrix production, and other metabolic profiles [6,12,35,39,45]. However, co-opting endogenous transduction targets for such purposes carries concerns regarding risks of physical cellular damage (e.g., mechanical loading approaches) and/or non-specific/off-target pharmacological side effects (e.g., small drug or biomolecular approaches) [49,50,76,77]. Instead, targeting Ca^{2+} activation through genomically-encoded, yet synthetic means can minimize such concerns while offering the precision needed to dissect the role of Ca^{2+} regulation in cartilage homeostasis, disease etiology, and tissue engineering/regeneration.

In pursuit of this goal, the present study demonstrated the facile ability to engineer the immortalized chondrocyte-like ATDC5 cell line to stably express the chemogenetic, CNO-responsive DREADD hM3Dq.

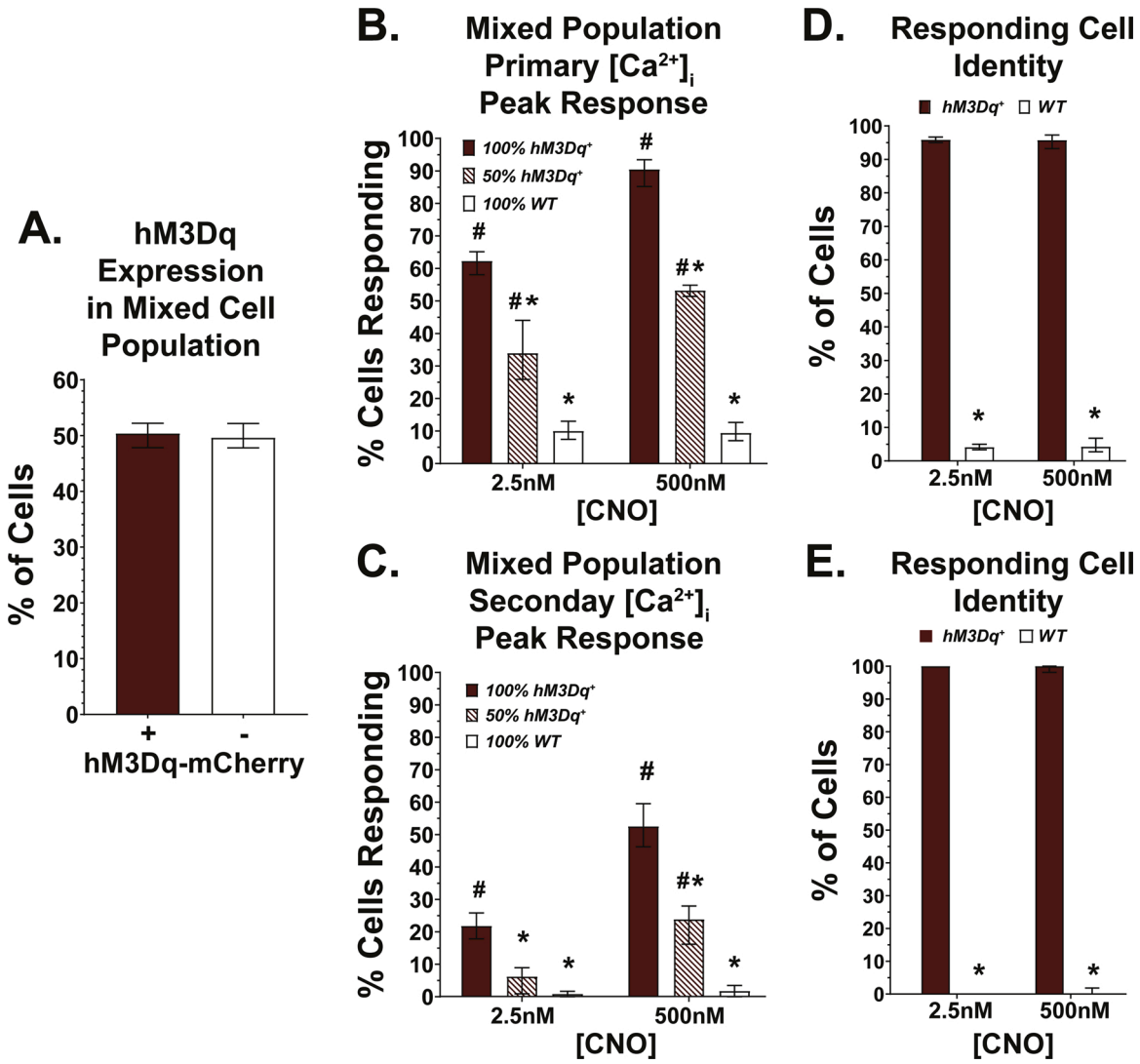

Fig. 6. CNO-evoked $[Ca^{2+}]_i$ signals in mixed expression cultures of $hM3Dq^+$ and WT ATDC5 cells (mixed 1:1). **A.** Visual quantification of $hM3Dq^+$ receptor expression confirmed ~50 % mCherry-hM3Dq expression in these mixed expression populations. Stimulation of mixed expression populations with CNO (2.5 or 500 nM) resulted in ~50 % reductions in the number cells exhibiting CNO-driven **B.** Primary $[Ca^{2+}]_i$ peaks and **C.** Secondary $[Ca^{2+}]_i$ peaks (each response was reduced to half of the 100 % $hM3Dq^+$ relative to the 100 % WT responses). **D & E.** Cells that responded to CNO in mixed expression cultures were almost exclusively $hM3Dq^+$; >95 % of responsive cells were $hM3Dq^+$, <5% of WT cells exhibited a single primary spontaneous $[Ca^{2+}]_i$ signal and <1% of WT cells exhibited two or more Ca^{2+} peaks. Data are presented as mean ± range; * indicates $p < 0.05$ compared to respective 100 % $hM3Dq^+$ control and # indicates $p < 0.05$ compared to respective 100 % WT control, one-way ANOVA.

This research built directly upon a prior study demonstrating the feasibility of synthetically activating the innate $G\alpha_q$-PLCβ-IP_3-ER pathway to drive $[Ca^{2+}]_i$ activation in ATDC5 cells via transiently-expressed hM3Dq and its ligand, CNO [51], while addressing limitations and gaps in knowledge associated with the preceding study. In our stable line, >97 % of lentivirally transduced cells expressed mCherry-hM3Dq, as confirmed by fluorescent imaging, with strong receptor presence at the plasma membrane and within punctate vesicles in the cell, in agreement with cellular targeting of hM3Dq and GPCRs [78]. The presence of less than perfect transduction efficiency in continuously selected cells might be attributable to limitations associated with fluorescent imaging-based confirmation [79] or genetic drift [80]; nonetheless, functional hM3Dq expression was robust, with >95 % of hM3Dq-transduced cells being responsive to CNO. Activation of $[Ca^{2+}]_i$ signaling in $hM3Dq^+$ ATDC5 cells occurred in a rapid, coordinated, and CNO dose-dependent manner. In contrast, non-transfected WT cells were irresponsive to CNO; all observed WT $[Ca^{2+}]_i$ activations were likely attributable to infrequent and spontaneous ion channel opening [81].

Our studies indicated an influence of temperature on primary $hM3Dq^+$ cell activation (a ~50 % lower primary $[Ca^{2+}]_i$ peak EC_{50} was observed at 37 °C compared to 25 °C, and faster Ca2+ signaling dynamics were seen). More interestingly though, $hM3Dq^+$ cells were more responsive to very-low concentration CNO (1−100pM) at 37 °C than at 25 °C, an effect not observed in unstimulated $hM3Dq^+$ or WT cells. This temperature-dependent elevation in $hM3Dq^+$ Ca^{2+} response at low CNO concentrations might be attributable to interactions between protein kinase C (PKC) and TRPV4. PKC is a kinase activated downstream of $G_{q\alpha}$-mediated signaling [54], while TRPV4 is a Ca^{2+}-permeable channel that mediates trans-membrane Ca^{2+} flux [72]. TRPV4 displays Boltzman's distribution-like activation at temperatures between 25 °C and 41 °C [82], and PKC-mediated phosphorylation of TRPV4 can shift its temperature sensitivity lower, resulting in 'heat hyperalgesia' [83]. One might speculate that sub-threshold hM3Dq activation—at agonist levels insufficient to drive $[Ca^{2+}]_i$ signaling through IP_3-mediated Ca^{2+} release—could potentially drive PKC-mediated TRPV4 sensitization [84,

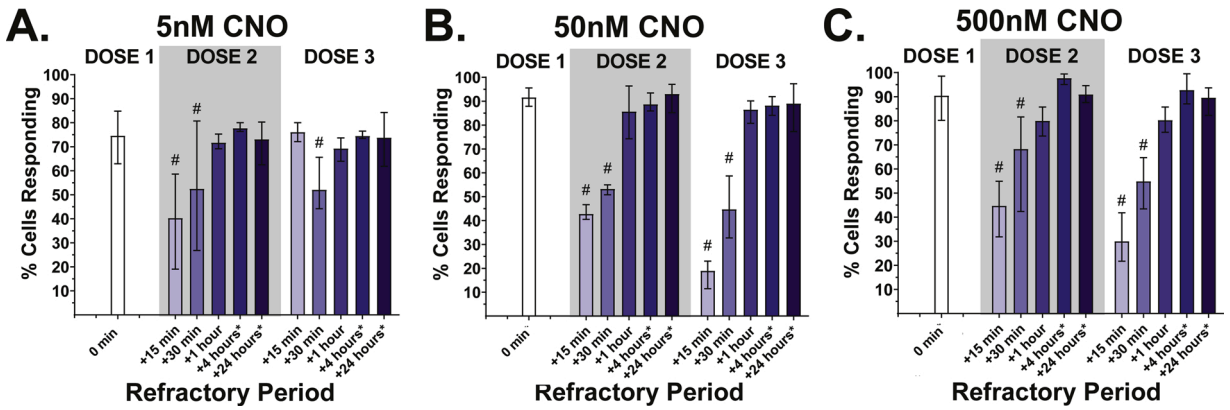

Fig. 7. Refractory behavior of CNO-mediated $[Ca^{2+}]_i$ signaling hM3Dq$^+$ ATDC5 cells. At 2, 20, and 200 times CNO's EC_{50} concentration, hM3Dq signaling fully recovered following 1 h of CNO washout (panels **A-C**, respectively). Note: the 4- and 24 -h refractory groups (*) were removed from the incubated microscope stage and placed in a 37°C cell culture incubator in-between CNO doses, and thus represent unpaired tests. Data are presented as mean ± range; Dose 1 is displayed as the average of all samples' 0 min values; # indicates $p < 0.05$ from the respective initial (0 min) baseline activation control; two-way ANOVA w/ Tukey post-hoc.

85]. The mechanisms underlying synergism between temperature and hM3Dq activation of $[Ca^{2+}]_i$, especially at low CNO concentration, represents an area of future study.

In quantifying hM3Dq$^+$-mediated $[Ca^{2+}]_i$ signaling kinetics, we identified an inverse relationship between CNO concentration and primary $[Ca^{2+}]_i$ peak duration and magnitude. At low CNO concentrations, Ca^{2+} peaks were typically less coordinated and longer in duration; as CNO concentration increased, peak duration decreased as a result of reductions in both signal rise and fall time, behaviors that were not observed for the secondary/oscillatory peaks. CNO-evoked primary $[Ca^{2+}]_i$ peak heights were, on average, double those of spontaneous WT $[Ca^{2+}]_i$ activations and their durations two to four times that of spontaneous $[Ca^{2+}]_i$ activations. Following primary peak generation, often extensive oscillatory Ca^{2+} signaling behaviors were observed (upwards of 60 % of cells), and with increasing secondary peak number oscillatory peak height and duration approached those of spontaneous WT $[Ca^{2+}]_i$ activations.

Through a battery of Ca^{2+} pathway inhibition studies we demonstrated that hM3Dq-evoked $[Ca^{2+}]_i$ signaling is primarily driven though IP_3-mediated Ca^{2+} release from intracellular ER stores and that otherwise infrequent and spontaneous $[Ca^{2+}]_i$ signaling in ATDC5 cells occurs independent of ER Ca^{2+} mobilization [25,86]. When the IP_3-pathway inhibitors, thapsigargin or U-73122, were administered coincident with CNO stimulation, initial hM3Dq-driven primary Ca^{2+} peaks were retained, but subsequent Ca^{2+} oscillations were blocked. Pre-inhibition abolished all hM3Dq-mediated signaling. Timed inhibition using Xestospongin C could not be performed due to the kinetics of its IP_3R antagonization [87]. While we fully expected hM3Dq-initiated Ca^{2+} signaling to be mediated by PLCβ-IP_3-controlled calcium release from the ER [59], several intracellular/autocrine signaling pathways have been implicated in calcium-induced calcium release and oscillatory Ca^{2+} signal generation in chondrocytes [2,3,88–90]. Our results indicate that neither individual inhibition of extracellularly-mediated ATP signaling, Ca^{2+} entry via extracellular pathways (through TRPV4, store-operated channels, or cation channels more generally), or PKC signaling influenced primary CNO-mediate $[Ca^{2+}]_i$ peak or secondary Ca^{2+} oscillation generation in hM3Dq$^+$ cells. Furthermore, suppression of extracellular calcium influx did not markedly alter the dynamics of CNO-mediated signaling (Supplemental Fig. 7). Only combinatorial inhibition of both ATP receptor classes diminished secondary Ca^{2+} peaks responses, an effect in line with ATP's role in sustaining Ca^{2+} oscillations but not in their initiation [43]. Furthermore, our mixed expression study elegantly and broadly confirmed that CNO-mediated $[Ca^{2+}]_i$ signaling was not driven by paracrine mechanisms.

$G\alpha_q$ protein activation also drives diacylglycerol (DAG) production, which activates membrane bound PKC [54]. Inhibition of PKC resulted in a modest, but non-significant reduction in CNO-evoked primary Ca^{2+} peaks, while blunting oscillatory signaling behaviors in hM3Dq$^+$ cells. This response was unlikely due to TRPV4 sensitization, as our inhibition studies confirm, but may reflect regulatory effects of PKCs on IP_3 oscillations in response to $[Ca^{2+}]_i$ [91,92]. These outcomes confirm that CNO-mediated Ca^{2+} signaling in hM3Dq$^+$ cells occurs solely through targeted activation of the $G\alpha_q$-PLCβ-IP_3-ER pathway, and that the resultant oscillatory Ca^{2+} signaling behaviors are regulated through a cell-autonomous interplay between $[Ca^{2+}]_i$ levels, PLCβ-mediated IP_3 generation, and PKC-mediated regulation of IP_3/PIP_2 recycling [93].

Lastly, studies of the long-term effects of hM3Dq-mediated Ca^{2+} signaling on ATDC5 cells (and other chondrogenic cells) requires the ability to repeatedly activate CNO-dependent Ca^{2+} signaling, and thus knowledge of the dosing frequencies under which fully reproducible Ca^{2+} activations can be elicited. In 2D culture, hM3Dq-evoked Ca^{2+} re-activation in ATDC5 cells was markedly attenuated for washout and re-challenges of less than 30-minutes, while near-full recovery of signaling was seen following one-hour CNO washout. These results suggest a refractory signaling period of ~1 h, which is consistent with $G\alpha_q$-GPCR recycling times and the kinetics of $G\alpha_q$-mediated signaling desensitization/re-sensitization and GPCR downregulation [94,95].

The hM3Dq platform described in the present study represents a novel tool for the study of IP_3-mediated calcium signaling influences on gene expression, protein secretion, and cellular behavior/health in ATDC5 cells, and to explore the use of chemogenetic regulation of $[Ca^{2+}]_i$, and GPCR signaling to synthetically control chondrocyte/cartilage physiology. While it is well established that mechanical stimulation of Ca^{2+} signaling is necessary for proper cartilage development, tissue engineering, and tissue homeostasis [96–98]; *ex vivo* application of mechanical stimulation can be both injurious and technically challenging to implement. Furthermore, when engineering cartilage tissues, an early adaptation phase, often lasting for weeks, is typically necessary, during which mechanical stimulation of the tissue scaffold risks the driving of cell death and catabolic responses that harm tissue development [76,94,95]. Alternatively, activation of $[Ca^{2+}]_i$ signaling through the use of exogenous ligands of chondrocyte calcium channels, such as the TRPV4 agonist GSK101, has been explored as non-invasive means to improve engineered cartilage maturation during this early adaptation phase [45]. However, targeting endogenous signal transducers carries risks of off-target effects, which may hinder acceptance when co-culture or *in vivo* modulation/regeneration strategies are being considered. Chemogenetic approaches hold promise in reducing these risks, as cells not engineered to express engineered receptors will be insensitive to the direct effects of its regulator. Thus, a platform like DREADDs may offer distinct advantages to i) shortening the cell adaptation phase in engineered hydrogels, ii) accelerating the maturation of engineered tissues,

and iii) reducing the risk of activating ubiquitous endogenous signaling pathways in off-target cells.

Despite the novelty of the present study, a number of limitations must be noted. First, ATDC5 is an immortalized chondroprogenitor cell line, not true primary chondrocytes or mesenchymal stem cells; studies of DREADD function within primary chondrocytes/chondroprogenitors will be necessary moving forward. Second, lentiviral transduction permits stable genomic integration, but no control over integration location, carrying risks of off-target insertional mutagenesis; future use of precision genetic engineering tools, such as CRISPR/Cas9, and conditional expression vectors should enable generation of cells with controlled and uniform integration, and expression levels. Thirdly, while CNO, the synthetic ligand of hM3Dq, is 'inert' *in vitro*, it can be 'reverse' metabolized into its precursor, clozapine, an antipsychotic drug, *in vivo*, resulting in behavioral effects [99]; use of alternative ligands, such as DREADD compound 21 [100], may limit these off-target/metabolic effects. Fourthly, the present study was restricted to the induction and regulation of $[Ca^{2+}]_i$ signaling in ATDC5 cells in 2D. Investigations of the influence of CNO-driven hM3Dq activation on both ATDC5 and primary cells in 2D (micromass) and 3D (micropellet/microtissue) culture are ongoing, and will focus on the ability of hM3Dq activation to promote cartilage-like matrix development and maturation in the absence and the presence of applied mechanical loading. Lastly, a limited number of studies, using mainly knock-out models, have shown the importance of $G\alpha_s$- and $G\alpha_q$-coupled signaling pathways in—predominately growth plate—chondrocyte biology [101, 102]. While the present study focused on $G\alpha_q$ signaling, DREADDs for $G\alpha_i$ and $G\alpha_s$-coupled GPCRs are available [59] and can be utilized to study the role of these signaling pathways on chondrocyte physiology. Nonetheless, the hM3Dq DREADD system reported here represents a unique platform to directly interrogate the influence of $G\alpha_q$-signaling and Ca^{2+} signaling on articular chondrocyte biology and cartilage health, homeostasis, and pathology, and represents a novel tool to direct towards improving the study and generation of tissue engineered/regenerated articular cartilage.

Author declaration

All authors have seen and approved the final article for submission. They warrant that the article is the authors' original work and is not under consideration for publication elsewhere.

CRediT authorship contribution statement

Ryan C. McDonough: Conceptualization, Investigation, Data curation, Software, Formal analysis, Methodology, Validation, Visualization, Writing - original draft, Writing - review & editing. **Rachel M. Gilbert:** Methodology, Validation, Writing - review & editing. **Jason P. Gleghorn:** Conceptualization, Resources, Methodology, Writing - review & editing. **Christopher Price:** Conceptualization, Project administration, Supervision, Resources, Methodology, Data curation, Formal analysis, Visualization, Writing - original draft, Writing - review & editing, Funding acquisition.

Declaration of Competing Interest

The authors report no declarations of interest.

Appendix A. Supplementary data

Supplementary material related to this article can be found, in the online version, at doi:https://doi.org/10.1016/j.ceca.2021.102363.

References

[1] J. Sanchez-Adams, H.A. Leddy, A.L. McNulty, C.J. O'Conor, F. Guilak, The mechanobiology of articular cartilage: bearing the burden of osteoarthritis, Curr. Rheumatol. Rep. 16 (10) (2014) 1–9, https://doi.org/10.1007/s11926-014-0451-6.

[2] D.E. Clapham, Calcium signaling, Cell 131 (6) (2007) 1047–1058, https://doi.org/10.1016/j.cell.2007.11.028.

[3] C. Matta, R. Zakany, Calcium signalling in chondrogenesis: implications for cartilage repair, Front. Biosci. (Schol. Ed.) 5 (January) (2013) 305–324, https://doi.org/10.1089/ten.TEB.2013.0757.

[4] J.D. San Antonio, R.S. Tuan, Chondrogenesis of limb bud mesenchyme in vitro: stimulation by cations, Dev. Biol. 115 (2) (1986) 313–324, https://doi.org/10.1016/0012-1606(86)90252-6.

[5] M. Tomita, M.I. Reinhold, J.D. Molkentin, M.C. Naski, Calcineurin and NFAT4 induce chondrogenesis, J. Biol. Chem. 277 (44) (2002) 42214–42218, https://doi.org/10.1074/jbc.C200504200.

[6] A.J. Steward, The role of calcium signalling in the chondrogenic response of mesenchymal stem cells to hydrostatic pressure, Eur. Cells Mater. 28 (2014) 358–371.

[7] O. Jacenko, R.S. Tuan, Chondrogenic potential of chick embryonic calvaria: I. Low calcium permits cartilage differentiation, Dev. Dyn. 202 (1995) 13–26, https://doi.org/10.1002/aja.1002020103.

[8] K. Gavenis, C. Schumacher, U. Schneider, J. Eisfeld, J. Mollenhauer, B. Schmidt-Rohlfing, Expression of ion channels of the TRP family in articular chondrocytes from osteoarthritic patients: changes between native and in vitro propagated chondrocytes, Mol. Cell. Biochem. 321 (2009) 135–143, https://doi.org/10.1007/s11010-008-9927-x.

[9] C.A.M. Huser, M.E. Davies, Calcium signaling leads to mitochondrial depolarization in impact-induced chondrocyte death in equine articular cartilage explants, Arthritis Rheum. 56 (7) (2007) 2322–2334, https://doi.org/10.1002/art.22717.

[10] R.M.L. La Rovere, G. Roest, G. Bultynck, J.B. Parys, Intracellular Ca2+ signaling and Ca2+ microdomains in the control of cell survival, apoptosis and autophagy, Cell Calcium 60 (2) (2016) 74–87, https://doi.org/10.1016/J.CECA.2016.04.005.

[11] C. Fewtrell, Ca2+ oscillations in non-excitable cells, Annu. Rev. Physiol. 55 (1) (1993) 427–454, https://doi.org/10.1146/annurev.ph.55.030193.002235.

[12] J.B. Fitzgerald, M. Jin, D. Dean, D.J. Wood, M.H. Zheng, A.J. Grodzinsky, Mechanical compression of cartilage explants induces multiple time-dependent gene expression patterns and involves intracellular calcium and cyclic AMP, J. Biol. Chem. 279 (19) (2004) 19502–19511, https://doi.org/10.1074/jbc.M400437200.

[13] I. Raizman, J.N.A. De Croos, R. Pilliar, R.A. Kandel, Calcium regulates cyclic compression-induced early changes in chondrocytes during in vitro cartilage tissue formation, Cell Calcium 48 (4) (2010) 232–242, https://doi.org/10.1016/j.ceca.2010.09.006.

[14] N. Trompeter, J. Gardinier, V. DeBarros, et al., Insulin-Like Growth Factor-1 Regulates the Mechanosensitivity of Chondrocytes by Modulating TRPV4, bioRxiv. 2020, 1950, pp. 1–29, https://doi.org/10.1101/2020.03.10.985713.

[15] M.J. Berridge, M.D. Bootman, H.L. Roderick, Calcium signalling: dynamics, homeostasis and remodelling, Nat. Rev. Mol. Cell Biol. 4 (7) (2003) 517–529, https://doi.org/10.1038/nrm1155.

[16] J.C. Sanchez, T.A. Danks, R.J. Wilkins, Mechanisms involved in the increase in intracellular calcium following hypotonic shock in bovine articular chondrocytes, Gen. Physiol. Biophys. 22 (4) (2003) 487–500.

[17] F. Guilak, R. Zell, G. Erickson, D. Grande, Mechanically induced calcium waves in articular chondrocytes are inhibited by gadolinium and amiloride, J. Orthop. Res. 17 (3) (1999) 421–429, https://doi.org/10.1002/jor.1100170319.

[18] B. Pingguan-Murphy, M. El-Azzeh, D.L. Bader, M.M. Knight, Cyclic compression of chondrocytes modulates a purinergic calcium signalling pathway in a strain rate- and frequency-dependent manner, J. Cell. Physiol. 209 (1) (2006) 389–397, doi:10.1002/JCP.

[19] M. Edlich, C.E. Yellowley, C.R. Jacobs, H.J. Donahue, Oscillating fluid flow regulates cytosolic calcium concentration in bovine articular chondrocytes, J. Biomech. 34 (2001) 59–65.

[20] F. Vincent, A. Acevedo, M.T. Nguyen, et al., Identification and characterization of novel TRPV4 modulators, Biochem. Biophys. Res. Commun. 389 (3) (2009) 490–494, https://doi.org/10.1016/j.bbrc.2009.09.007.

[21] K. Shibasaki, TRPV4 activation by thermal and mechanical stimuli in disease progression, Lab Invest. (2020), https://doi.org/10.1038/s41374-019-0362-2. Published online.

[22] E.R. Horwitz, T.M. Higgins, B.J. Harvey, Histamine-induced cytosolic calcium increase in porcine articular chondrocytes, Biochim. Biophys. Acta – Mol. Cell Res. 1313 (2) (1996) 95–100, https://doi.org/10.1016/0167-4889(96)00057-2.

[23] M.K. Elfervig, R.D. Graff, G.M. Lee, S.S. Kelley, A. Sood, A.J. Banes, ATP induces Ca2+ signaling in human chondrons cultured in three-dimensional agarose films, Osteoarthr. Cartil. 9 (6) (2001) 518–526, https://doi.org/10.1053/joca.2000.0435.

[24] R. Parekh, A. Clark, Transforming growth factor-β elicits a calcium response in chondrocytes ex vivo, Osteoarthr. Cartil. 21 (2013) S134, https://doi.org/10.1016/j.joca.2013.02.283.

[25] Y. Zhou, M. Lv, T. Li, et al., Spontaneous calcium signaling of cartilage cells: from spatiotemporal features to biophysical modeling, FASEB J. 33 (4) (2019) 4675–4687, https://doi.org/10.1096/fj.201801460R.

[26] B. Ye, Ca2+ oscillations and its transporters in mesenchymal stem cells, Physiol. Res. 59 (3) (2010) 323–329.

[27] T. Tomida, K. Hirose, A. Takizawa, F. Shibasaki, M. Iino, NFAT functions as a working memory of Ca2+ signals in decoding Ca2+ oscillation, EMBO J. 22 (15) (2003) 3825–3832, https://doi.org/10.1093/emboj/cdg381.

[28] R.E. Dolmetsch, K. Xu, R.S. Lewis, Calcium oscillations increase the efficiency and specificity of gene expression, Nature 392 (6679) (1998) 933–936, https://doi.org/10.1038/31960.

[29] P.G. Hogan, L. Chen, J. Nardone, A. Rao, Transcriptional regulation by calcium, calcineurin, and NFAT, Genes Dev. 17 (2003) 2205–2232, https://doi.org/10.1101/gad.1102703.

[30] A. Argentaro, H. Sim, S. Kelly, et al., A SOX9 defect of calmodulin- dependent nuclear import in campomelic dysplasia/autosomal sex reversal, J. Biol. Chem. 278 (36) (2003) 33839–33847, https://doi.org/10.1074/jbc.M302078200.

[31] I. Uzieliene, P. Bernotas, A. Mobasheri, E. Bernotiene, The role of physical stimuli on calcium channels in chondrogenic differentiation of mesenchymal stem cells, Int. J. Mol. Sci. 19 (10) (2018) 2998, https://doi.org/10.3390/ijms19102998.

[32] M. Mardani, S. Roshankhah, B. Hashemibeni, M. Salahshoor, E. Naghsh, E. Esfandiari, Induction of chondrogenic differentiation of human adipose-derived stem cells by low frequency electric field, Adv. Biomed. Res. 30 (5) (2016) 97, https://doi.org/10.4103/2277-9175.183146.

[33] H.J. Kwon, G.S. Lee, H. Chun, Electrical stimulation drives chondrogenesis of mesenchymal stem cells in the absence of exogenous growth factors, Sci. Rep. 6 (2016), https://doi.org/10.1038/srep39302.

[34] S.-S. Lin, B.-H. Tzeng, K.-R. Lee, R.J.H. Smith, K.P. Campbell, C.-C. Chen, Cav3.2 T-type calcium channel is required for the NFAT-dependent Sox9 expression in tracheal cartilage, PNAS 111 (19) (2014) E1990–E1998, https://doi.org/10.1073/pnas.1323112111.

[35] C.L. Gilchrist, H.A. Leddy, L. Kaye, et al., TRPV4-mediated calcium signaling in mesenchymal stem cells regulates aligned collagen matrix formation and vinculin tension, Proc. Natl. Acad. Sci. U. S. A. 116 (6) (2019) 1992–1997, https://doi.org/10.1073/pnas.1811095116.

[36] X. Gong, W. Xie, B. Wang, et al., Altered spontaneous calcium signaling of in situ chondrocytes in human osteoarthritic cartilage, Sci. Rep. 7 (1) (2017) 1–12, https://doi.org/10.1038/s41598-017-17172-w.

[37] Y. Zhou, M. Park, E. Cheung, L. Wang, X.L. Lu, The effect of chemically defined medium on spontaneous calcium signaling of in situ chondrocytes during long-term culture, J. Biomech. 48 (6) (2015) 990–996.

[38] M. Lv, Y. Zhou, X. Chen, L. Han, L. Wang, X.L. Lu, Calcium signaling of in situ chondrocytes in articular cartilage under compressive loading: roles of calcium sources and cell membrane ion channels, J. Orthop. Res. (2017), https://doi.org/10.1002/jor.23768. Published online October 5.

[39] J.F. Weber, S.D. Waldman, Calcium signaling as a novel method to optimize the biosynthetic response of chondrocytes to dynamic mechanical loading, Biomech. Model. Mechanobiol. 13 (6) (2014) 1387–1397, https://doi.org/10.1007/s10237-014-0580-x.

[40] S. Kawano, S. Shoji, S. Ichinose, K. Yamagata, M. Tagami, M. Hiraoka, Characterization of Ca2+ signaling pathways in human mesenchymal stem cells, Cell Calcium 32 (4) (2002) 165–174, https://doi.org/10.1016/S0143416002001240.

[41] C. Matta, A. Mobasheri, Regulation of chondrogenesis by protein kinase C: emerging new roles in calcium signalling, Cell. Signal. 26 (5) (2014) 979–1000, https://doi.org/10.1016/J.CELLSIG.2014.01.011.

[42] M.D. Bootman, Calcium signaling, Cold Spring Harb. Perspect. Biol. 4 (2012) 1–3. http://www.ncbi.nlm.nih.gov/pubmed/18083096.

[43] S. Kawano, K. Otsu, A. Kuruma, et al., ATP autocrine/paracrine signaling induces calcium oscillations and NFAT activation in human mesenchymal stem cells, Cell Calcium 39 (4) (2006) 313–324, https://doi.org/10.1016/j.ceca.2005.11.008.

[44] Z. VArga, T. Juhasz, C. Matta, J. Fodor, Switch of voltage-gated K+ channel expression in the plasma membrane of chondrogenic cells affects cytosolic Ca2+-oscillations and cartilage formation, PLoS One 6 (11) (2011) 27957, https://doi.org/10.1371/journal.pone.0027957.

[45] C.J. O'Conor, H.A. Leddy, H.C. Benefield, W.B. Liedtke, F. Guilak, TRPV4-mediated mechanotransduction regulates the metabolic response of chondrocytes to dynamic loading, Proc. Natl. Acad. Sci. U. S. A. 111 (4) (2014) 1316–1321, https://doi.org/10.1073/pnas.1319569111.

[46] A.L. McNulty, H.A. Leddy, W. Liedtke, F. Guilak, TRPV4 as a therapeutic target for joint diseases, Naunyn Schmiedebergs Arch. Pharmacol. 388 (4) (2015) 437–450, https://doi.org/10.1007/s00210-014-1078-x.

[47] A. Mobasheri, P. Martín-Vasallo, Epithelial sodium channels in skeletal cells; a role in mechanotransduction? Cell Biol. Int. 23 (4) (1999) 237–240, https://doi.org/10.1006/cbir.1999.0405.

[48] M. Nagao, S. Ishii, H. Yabu, Voltage-gated ionic channels in cultured rabbit articular chondrocytes, Comp. Biochem. Physiol. Part C Pharmacol. Toxicol. Endocrinol. 115 (3) (1996) 223–232, https://doi.org/10.1016/S0742-8413(96)00091-6.

[49] J. Vriens, G. Appendino, B. Nilius, Pharmacology of vanilloid transient receptor potential cation channels, Mol. Pharmacol. 75 (6) (2009) 1262–1279, https://doi.org/10.1124/mol.109.055624.

[50] A. Rojas, M. Padidam, D. Cress, W.M. Grady, TGF-beta receptor levels regulate the specificity of signaling pathway activation and biological effects of TGF-beta, Biochim. Biophys. Acta 1793 (7) (2009) 1165–1173, https://doi.org/10.1016/j.bbamcr.2009.02.001.

[51] R.C. McDonough, J.S. Shoga, C. Price, DREADD-based synthetic control of chondrocyte calcium signaling in vitro, J. Orthop. Res. 37 (7) (2019) 1518–1529, https://doi.org/10.1002/jor.24285.

[52] B.N. Armbruster, X. Li, M.H. Pausch, S. Herlitze, B.L. Roth, Evolving the lock to fit the key to create a family of G protein-coupled receptors potently activated by an inert ligand, Proc. Natl. Acad. Sci. U. S. A. 104 (12) (2007) 5163–5168, https://doi.org/10.1073/pnas.0700293104.

[53] R.S. Prosser, T.H. Kim, G protein-coupled receptors in drug discovery, Methods Mol. Biol. 1335 (2015) 39–51, https://doi.org/10.1007/978-1-4939-2914-6.

[54] N. Tuteja, Signaling through G protein coupled receptors, Plant Signal. Behav. 4 (10) (2009) 942–947, https://doi.org/10.4161/psb.4.10.9530.

[55] R. Leurs, R.A. Bakker, H. Timmerman, I.J.P. de Esch, The histamine H3 receptor: from gene cloning to H3 receptor drugs, Nat. Rev. Drug Discov. (2005), https://doi.org/10.1038/nrd1631. Published online.

[56] J. Li, Y. Ning, W. Hedley, et al., The molecule pages database, Nature (2002), https://doi.org/10.1038/nature01307. Published online.

[57] K.S. Smith, D.J. Bucci, B.W. Luikart, S.V. Mahler, DREADDs: use and application in behavioral neuroscience, Behav. Neurosci. (2016), https://doi.org/10.1037/bne0000135. Published online.

[58] H. Zhu, B.L. Roth, DREADD: a chemogenetic GPCR signaling platform, Int. J. Neuropsychopharmacol. 18 (1) (2014), https://doi.org/10.1093/ijnp/pyu007.

[59] S.C. Rogan, B.L. Roth, Remote control of neuronal signaling, Pharmacol. Rev. 63 (2) (2011) 291–315, https://doi.org/10.1124/pr.110.003020.

[60] M.J. Berridge, The inositol trisphosphate/calcium signaling pathway in health and disease, Physiol. Rev. 96 (4) (2016) 1261–1296, https://doi.org/10.1152/physrev.00006.2016.

[61] R. Barrett-Jolley, R. Lewis, R. Fallman, A. Mobasheri, The emerging chondrocyte channelome, Front. Physiol. 1 (135) (2010) 1–11, https://doi.org/10.3389/fphys.2010.00135.

[62] M. Grundmann, E. Kostenis, Temporal bias: time-encoded dynamic GPCR signaling the temporal dimension of G-protein-coupled receptor signaling, Trends Pharmacol. Sci. 38 (12) (2017) 1110–1124, https://doi.org/10.1016/j.tips.2017.09.004.

[63] G.M. Alexander, S.C. Rogan, A.I. Abbas, et al., Remote control of neuronal activity in transgenic mice expressing evolved G protein-coupled receptors, Neuron 63 (1) (2009) 27–39, https://doi.org/10.1016/j.neuron.2009.06.014. Remote.

[64] M.J. Krashes, S. Koda, C. Ye, et al., Rapid, reversible activation of AgRP neurons drives feeding behavior in mice, J. Clin. Invest. 121 (4) (2011) 1424–1428, https://doi.org/10.1172/JCI46229.

[65] S. Jain, I.R. De Azua, H. Lu, M.F. White, J.M. Guettier, J. Wess, Chronic activation of a designer Gq-coupled receptor improves β cell function, J. Clin. Invest. 123 (4) (2013) 1750–1762, https://doi.org/10.1172/JCI66432.

[66] J. Hua Li, S. Jain, S.M. McMillin, et al., A novel experimental strategy to assess the metabolic effects of selective activation of a G q - coupled receptor in hepatocytes in vivo, Endocrinology 154 (10) (2013) 3539–3551, https://doi.org/10.1210/en.2012-2127.

[67] A. Kaufmann, A. Keim, G. Thiel, Regulation of immediate-early gene transcription following activation of Gq-coupled designer receptors, J. Cell. Biochem. 114 (3) (2013) 681–696, https://doi.org/10.1002/jcb.24410.

[68] J.C. Sánchez, T.A. Danks, R.J. Wilkins, R.J. Wilkins, Mechanisms involved in the increase in intracellular calcium following hypotonic shock in bovine articular chondrocytes, Gen. Physiol. Biophys. 22 (4) (2003) 487–500.

[69] Y. Shibukawa, T. Suzuki, Ca2+ signaling mediated by IP3-dependent Ca2+ releasing and store-operated Ca2+ channels in rat odontoblasts, J. Bone Miner. Res. 18 (1) (2003) 30–38, https://doi.org/10.1359/jbmr.2003.18.1.30.

[70] H.J. Motulsky, R.E. Brown, Detecting outliers when fitting data with nonlinear regression - a new method based on robust nonlinear regression and the false discovery rate, BMC Bioinform. (2006), https://doi.org/10.1186/1471-2105-7-123. Published online.

[71] S.-K. Han, W. Wouters, A. Clark, W. Herzog, Mechanically induced calcium signaling in chondrocytes in situ, J. Orthop. Res. 30 (3) (2012) 475–481, https://doi.org/10.1002/jor.21536.

[72] X. Gao, L. Wu, R.G. O'Neil, Temperature-modulated diversity of TRPV4 channel gating: activation by physical stresses and phorbol ester derivatives through protein kinase C-dependent and -independent pathways, J. Biol. Chem. 278 (29) (2003) 27129–27137, https://doi.org/10.1074/jbc.M302517200.

[73] E. Mariani, L. Pulsatelli, A. Facchini, Signaling pathways in cartilage repair, Int. J. Mol. Sci. 15 (5) (2014) 8667–8698, https://doi.org/10.3390/ijms15058667.

[74] S.D. Waldman, D.C. Couto, M.D. Grynpas, R.M. Pilliar, R.A. Kandel, A single application of cyclic loading can accelerate matrix deposition and enhance the properties of tissue-engineered cartilage, Osteoarthr. Cartil. 14 (4) (2006) 323–330, https://doi.org/10.1016/j.joca.2005.10.007.

[75] G.N. Bancroft, V.I. Sikavitsas, J. van den Dolder, et al., Fluid flow increases mineralized matrix deposition in 3D perfusion culture of marrow stromal osteoblasts in a dose-dependent manner, Proc. Natl. Acad. Sci. U. S. A. 99 (20) (2002) 12600–12605, https://doi.org/10.1073/pnas.202296599.

[76] E.G. Lima, L. Bian, K.W. Ng, et al., The beneficial effect of delayed compressive loading on tissue-engineered cartilage constructs cultured with TGF-beta3, Osteoarthr. Cartil. 15 (9) (2007) 1025–1033, https://doi.org/10.1016/j.joca.2007.03.008.

[77] C.A. Vilela, C. Correia, J.M. Oliveira, R.A. Sousa, J. Espregueira-Mendes, R. L. Reis, Cartilage repair using hydrogels: a critical review of in vivo experimental designs, ACS Biomater. Sci. Eng. 1 (2015) 726–739, https://doi.org/10.1021/acsbiomaterials.5b00245.

[78] D.M. Rosenbaum, S.G.F. Rasmussen, B.K. Kobilka, The structure and function of G-protein-coupled receptors, Nature 2 459 (7245) (2014) 356–363, https://doi.org/10.1038/nature08144.

[79] E.H.K. Stelzer, Contrast, resolution, pixelation, dynamic range and signal-to-noise ratio: fundamental limits to resolution in fluorescence light microscopy, J. Microsc. 189 (1) (1998) 15–24, https://doi.org/10.1046/j.1365-2818.1998.00290.x.
[80] R.F. Shearer, D.N. Saunders, Experimental design for stable genetic manipulation in mammalian cell lines: lentivirus and alternatives, Genes Cells 20 (1) (2015) 1–10, https://doi.org/10.1111/gtc.12183.
[81] A.D. Güler, H. Lee, T. Iida, I. Shimizu, M. Tominaga, M. Caterina, Heat-evoked activation of the ion channel, TRPV4, J. Neurosci. 1 (22) (2002) 6408–6412, https://doi.org/10.1523/jneurosci.22-15-06408.2002.
[82] N. Mundt, M. Spehr, P.V. Lishko, TRPV4 is the temperature-sensitive ion channel of human sperm, Elife (2018), https://doi.org/10.7554/eLife.35853. Published online.
[83] J. Mercado, R. Baylie, M.F. Navedo, et al., Local control of TRPV4 channels by AKAP150-targeted PKC in arterial smooth muscle, J. Gen. Physiol. 143 (5) (2014) 559–575, https://doi.org/10.1085/jgp.201311050.
[84] S. Manita, W.N. Ross, IP3 mobilization and diffusion determine the timing window of CA2+ release by synaptic stimulation and a spike in rat CA1 pyramidal cells, Hippocampus 20 (4) (2010) 524–539, https://doi.org/10.1002/hipo.20644.
[85] J. Fernandes, I.M. Lorenzo, Y.N. Andrade, et al., IP3 sensitizes TRPV4 channel to the mechano-and osmotransducing messenger 5'-6'-epoxyeicosatrienoic acid, J. Cell Biol. 181 (1) (2008) 143–155, https://doi.org/10.1083/jcb.200712058.
[86] Y. Zhou, M.A. David, X. Chen, et al., Effects of osmolarity on the spontaneous calcium signaling of in situ juvenile and adult articular chondrocytes, Ann. Biomed. Eng. 44 (4) (2016) 1138–1147, https://doi.org/10.1007/s10439-015-1406-4.
[87] T. Oka, K. Sato, M. Hori, H. Ozaki, H. Karaki, Xestospongin C, a novel blocker of IP3 receptor, attenuates the increase in cytosolic calcium level and degranulation that is induced by antigen in RBL-2H3 mast cells, Br. J. Pharmacol. 135 (8) (2002) 1959–1966, https://doi.org/10.1038/sj.bjp.0704662.
[88] S. Pritchard, F. Guilak, Effects of interleukin-1 on calcium signaling and the increase of filamentous actin in isolated and in situ articular chondrocytes, Arthritis Rheum. 54 (7) (2006) 2164–2174, https://doi.org/10.1002/art.21941.
[89] G.W. Zamponi, K.P.M. Currie, Regulation of CaV2 calcium channels by G protein coupled receptors, Biochim. Biophys. Acta Biomembr. 1828 (7) (2013) 1629–1643, https://doi.org/10.1016/J.BBAMEM.2012.10.004.
[90] L.H. Tse, Y.H. Wong, GPCRs in autocrine and paracrine regulations, Front. Endocrinol. (Lausanne) 10 (428) (2019) 1–11, https://doi.org/10.3389/fendo.2019.00428.
[91] P.J. Bartlett, W. Metzger, L.D. Gaspers, A.P. Thomas, Differential regulation of multiple steps in inositol 1,4,5-trisphosphate signaling by protein kinase C shapes hormone-stimulated Ca2+ oscillations, J. Biol. Chem. 290 (30) (2015) 18519–18533, https://doi.org/10.1074/jbc.M115.657767.
[92] H. Sipma, L. van der Zee, J. van den Akker, A. den Hertog, A. Nelemans, The effect of the PKC inhibitor GF109203X on the release of Ca2+ from internal stores and Ca2+ entry in DDT1 MF-2 cells, Br. J. Pharmacol. 119 (1996) 730–736. https://www.ncbi.nlm.nih.gov/pmc/articles/PMC1915768/pdf/brjpharm00073-0127.pdf.
[93] S. Thore, O. Dyachok, E. Gylfe, A. Tengholm, Feedback activation of phospholipase C via intracellular mobilization and store-operated influx of Ca2+ in insulin-secreting β-cells, J. Cell. Sci. 118 (19) (2005) 4463–4471, https://doi.org/10.1242/jcs.02577.
[94] N.J. Pavlos, P.A. Friedman, GPCR signaling and trafficking: the long and short of it, Trends Endocrinol. Metab. 28 (3) (2017) 213–226, https://doi.org/10.1016/j.tem.2016.10.007.
[95] F. Jean-Alphonse, A.C. Hanyaloglu, Regulation of GPCR signal networks via membrane trafficking, Mol. Cell. Endocrinol. 331 (2) (2011) 205–214, https://doi.org/10.1016/j.mce.2010.07.010.
[96] M.D. Buschmann, Y.A. Gluzband, A.J. Grodzinsky, E.B. Hunziker, Mechanical compression modulates matrix biosynthesis in chondrocyte/agarose culture, J. Cell Sci. 108 (Pt. 4) (1995) 1497–1508. http://www.ncbi.nlm.nih.gov/pubmed/7615670.
[97] M.B. Goldring, Chondrogenesis, chondrocyte differentiation, and articular cartilage metabolism in health and osteoarthritis, Ther. Adv. Musculoskelet. Dis. 4 (4) (2012) 269–285, https://doi.org/10.1177/1759720X12448454.
[98] R.L. Mauck, M.A. Soltz, C.C.B. Wang, et al., Functional tissue engineering of articular cartilage through dynamic loading of chondrocyte-seeded agarose gels, J. Biomech. Eng. 122 (3) (2000) 252, https://doi.org/10.1115/1.429656.
[99] D.F. Manvich, K.A. Webster, S.L. Foster, et al., The DREADD agonist clozapine N-oxide (CNO) is reverse-metabolized to clozapine and produces clozapine-like interoceptive stimulus effects in rats and mice, Sci. Rep. 8 (1) (2018) 3840, https://doi.org/10.1038/s41598-018-22116-z.
[100] M. Jendryka, M. Palchaudhuri, D. Ursu, et al., Pharmacokinetic and pharmacodynamic actions of clozapine-N-oxide, clozapine, and compound 21 in DREADD-based chemogenetics in mice, Sci. Rep. 9 (1) (2019) 4522, https://doi.org/10.1038/s41598-019-41088-2.
[101] A.S. Chagin, H.M. Kronenberg, Role of G-proteins in the differentiation of epiphyseal chondrocytes, J. Mol. Endocrinol. 53 (2) (2014) R39–R45, https://doi.org/10.1530/JME-14-0093.
[102] A.S. Chagin, K.K. Vuppalapati, T. Kobayashi, et al., G-protein stimulatory subunit alpha and Gq/11alpha G-proteins are both required to maintain quiescent stem-like chondrocytes, Nat. Commun. 5 (2014) 3673, https://doi.org/10.1038/ncomms4673.